

A New Chi-square Distribution De-noising Method for Image Encryption

Lin Teng, Hang Li, Shoulin Yin, and Yang Sun

(*Corresponding author: Hang Li and Shoulin Yin)

Software College, Shenyang Normal University

Shenyang 110034, China

(Email: lihansoft@163.com, 352720214@qq.com)

(Received Mar. 28, 2018; Revised and Accepted June 15, 2018; First Online June 15, 2019)

Abstract

In order to protect the security of the image, it is necessary to encrypt image and process domain image. Therefore, this paper proposes a new encryption domain image processing algorithms, image is encrypted using a sub-block scrambling pixel location algorithm. Then the image is denoised. Considering a given noisy image, the selection of thresholds should significantly affect the quality of the de-noising image. Although the state-of-the-art wavelet image de-noising methods perform better than other de-noising methods, they are not very effective for de-noising with different noise and with redundancy convergence time, sometimes. To mitigate the poor effect of traditional de-noising methods, this paper proposes a new wavelet soft threshold based on the Chi-square distribution-Kernel method. The Chi-square distribution-Kernel (CSDK) model is constructed to find the customized threshold that corresponds to the de-noised image. Then, the image receiver gets the decrypted image using the key restored pixel location. Finally, experimental results illustrate that this computationally scalable algorithm achieves state-of-the-art de-noising performance. The encryption results are also better.

Keywords: Chi-square Distribution-Kernel; Decryption; Image De-noising; Image Encryption

1 Introduction

In order to protect the security of the image [16, 27], to prevent leakage of image content, especially for military medical images, encryption processing is required. The image can take advantage of the existing image encryption algorithms to encrypt image and guarantee the security of the image. But it needs to compress, denoise the original image. If there are a lot of images, it provides to the third party equipment for processing that can significantly improve processing efficiency.

Cloud has attracted widespread attention and recogni-

tion as it transfers the traditional computing and storage functions into the cloud environment, which saves lots of hardware cost for users [18, 30]. With the development of cloud, more sensitive information (such as medical records, financial information and important documents of company) are stored in cloud [12, 19, 28]. Once the data are received by cloud provider, users lose the directly control for their data, which can cause the leak of privacy data. Encryption is an effective method to protect privacy of users' data. However, this way loses many features and can lead to difficult encryption [5, 6]. Especially, how to conduct encrypted data query in untrusted cloud environment has aroused people's attention.

During the process of image formation, transmission and processing, images are interfered by noise. Thus, the quality of the image can decrease. To remove or suppress the noise in the image and improve the image quality, many de-noising methods are proposed, such as linear and nonlinear filtering, spectral analysis, and multi-resolution analysis. However, these traditional methods largely depend on explicit or implicit assumptions to properly separate the true signal from the random noise. Over the past decade, wavelet analysis in the time domain and frequency domain, which has good localization properties and the multi-resolution analysis characteristics, has received much attention from researchers in different areas, including pattern recognition, image de-noising, signal processing and image compression. The wavelet analysis can effectively distinguish useful signal and noise, so it has become a notably effective image de-noising method.

At present, wavelet de-noising mainly includes three methods. First, it adopts the wavelet's singularity detection features to separate the signal and the noise. Second, it uses a wavelet coefficient threshold function to reduce the image noise. Third, the Bayesian criterion coefficient of the wavelet domain is used for image noise reduction. The wavelet threshold shrinkage method is the most widely used in image de-noising because of its simplicity and effectiveness.

The idea of wavelet threshold processing is derived

from the Donoho theory. Donoho first provided the general threshold de-noising formula based on an orthogonal wavelet transform, which made the complex de-noising problem easy to solve. However, because of the lack of adaptability of the scale space, the threshold is difficult to determine. The result can lead to fuzzy image edge and poor de-noising performance. Thus, many scholars have introduced different wavelet coefficient scales and their corresponding threshold to reduce image noise, such as the hard threshold, soft threshold [23], VisuShrink threshold [3], improved sub-band adaptive SureShrink threshold [8] and NormalShrink threshold [7]. Although these de-noising algorithms can obtain good de-noising effect, much detail information is eliminated.

The image quality seriously declines, and the pseudo Gibbs phenomenon may even be generated. To date, Wang [24] proposed an optimized shape parameter method for image de-noising. Kadhim [15] presented a Particle Swarm Optimization (PSO) algorithm to estimate the threshold value with no prior knowledge for these distributions. This process was achieved by implementing the PSO algorithm for kurtosis measuring of the residual noise signal to find an optimal threshold value, where the kurtosis function is maximal.

Ji [14] proposed a de-noising algorithm using the wavelet threshold method and exponential adaptive window width-fitting. His method was divided into three parts. First, the wavelet threshold method was used to filter the white noise. Second, the data were segmented using a data window. Then, an exponential fitting algorithm was used to fit the attenuation curve of each window, and the data polluted by non-stationary electromagnetic noise were replaced with their fitting results.

These methods have produced good effects for image de-noising, but few works aim to improve the threshold function, or their threshold functions are not better. Thus, we propose a new wavelet threshold function based on the Chi-square distribution-Kernel function for image de-noising. We also propose to consider shape parameters on the wavelet coefficients to be thresholded. Hence, the soft transformation can achieve a high precision of the true signal until the noise is commendably separated by shrinkage. To evaluate the performance of our new function, experiments were conducted on MATLAB to compare with other state-of-the-art methods. The results show that our new method performs better than other functions in terms of de-noising precision. Furthermore, the new function can enhance the image de-noising efficiency without the effect of layers or the number of image decompositions. New method can effectively remove noise and preserves the image details for de-noising image.

The remainder of this paper is organized as follows. The Preliminaries are presented in Section 2. Section 3 illustrates the new threshold based on CSDK in detail, and Section 4 presents the experimental results. The paper is concluded in Section 5.

2 Preliminaries

The presence of Gaussian white noise degrades images significantly and may hide important details and background on the images, leading to the loss of crucial information of original images. Traditionally, the first step toward removing related noise in images is to understand its statistical properties. Despite the theoretical appeal and the analytical simplicity of the Gaussian model, images of some natural scenes such as fog deviate from the Gaussian distribution. To mitigate this situation, various distributions such as the Weibull distribution [10], the log-normal distribution [1], the k-distribution [26] and Cauchy distribution [25] have been suggested.

However, in the above distributions, the log-normal distribution provides a convenient choice, but fails in modeling the lower half of the image histograms and overestimates the range of variation. Weibull distribution is an empirical model with limited theoretical justification. K-distribution is a successful model for SAR image despeckling, but not for this paper's testing data. Meanwhile, Generalised Cauchy distribution (GCD) is a symmetric distribution with bell-shaped density function as the Gaussian distribution but with a greater probability mass in the tails. GCD is a peculiar distribution due to the difficulty of estimating its location parameter and its heavy tail. Because it has no mean, variance or higher moments defined, GCD has a long convergence time. To alleviate the above problems, this paper utilizes Chi-square distribution-Kernel method for image de-noising. The following is illustration for Chi-square distribution.

Supposing that n independent random variables (ξ_1, \dots, ξ_n) obey the Gaussian distribution, its sum of squares $Q = \sum_{i=1}^n \xi_i^2$ composes of a new random variable, which is named the Chi-square distribution, where n is the freedom degree [4, 11]. The probability density function (PDF) of the Chi-square distribution is described as:

$$f(PDF) = \begin{cases} \frac{(1/2)^{n/2}}{\Gamma(n/2)} x^{(n/2)-1} e^{-x/2}, & \text{if } x \geq 0 \\ 0, & \text{otherwise} \end{cases}$$

The cumulative distribution function (CDF) $F_n(x)$ of the Chi-square distribution is defined as,

$$F_n(x) = \frac{\gamma(n/2, x/2)}{\Gamma(n/2)}$$

where $\Gamma(n/2, x/2)$ and $\gamma(k/2)$ are Gamma function and incomplete Gamma function, respectively.

3 Image Encryption and New De-noising Method

3.1 Image Encryption

In this paper, we use sub-block scrambling pixel location algorithm to encrypt the images. Assuming that size of

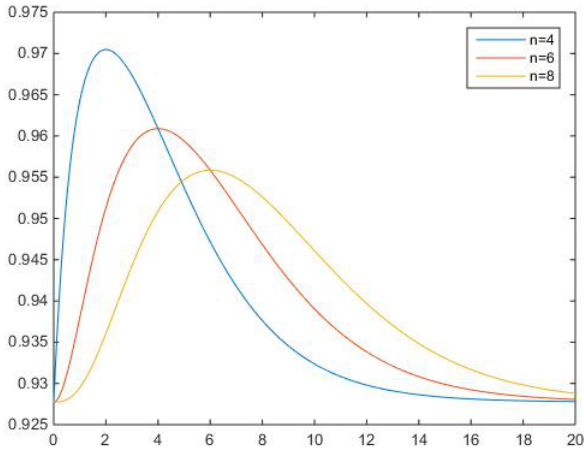


Figure 1: CSDK function with different n

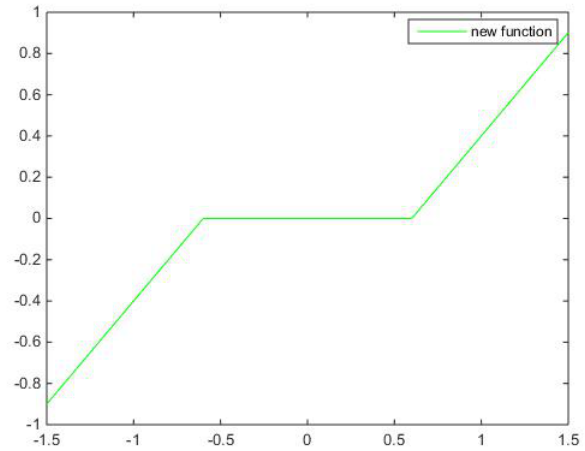


Figure 2: Wavelet soft thresholding based on CSDK

grayscale image I is $M \times N$. First, the image is divided into small patches (size is $S \times S$, number is $\lceil \frac{M}{S} \rceil \times \lceil \frac{N}{S} \rceil$) without overlap. Second, And then, places of these small patches are messed up. Under key controlling, the patch in (m,n) is moved to m', n' . Finally, for each piece, pixels are scrambled using the key within the block. Because the locations of the original image pixels are disrupted, who wants to know the image content will need to have the key. Through the encryption process, it can well protect the security and privacy of images.

3.2 Chi-square Distribution-Kernel Model Construction

The main hypothesis of our chi-square distribution-kernel model is that a combination of the structure Gaussian kernel of an image can significantly improve its reconstruction. The Gaussian kernel function has three important properties, which are conducive to image post-processing.

The Gaussian kernel function [2] can be written as:

$$y = \varepsilon e^{-\frac{(x-\mu)^2}{2\sigma^2}}$$

where $\varepsilon = 1$ is the height of the function; μ is the center of curve in the x-axis; σ is the width.

Based on the principle of the Gaussian kernel function, we construct the Chi-square Distribution-Kernel Model (CSDK). The new function $\mathfrak{R}(x)$ is summarized as:

$$\mathfrak{R}(x) = e^{-\frac{(1/((n/4) \int_0^\infty e^{-x} dx)(n/x^2-1)e^{-x/2-\mu})^2}{2\sigma^2}}$$

In $\mathfrak{R}(x)$, $n > 0$ is defined as the torsion resistance; μ and σ are the shape parameters. If n varies, $\mathfrak{R}(x)$ will change as shown in Figure 1. Figure 1 shows that the CSDK retains the better properties of the Chi-square distribution.

3.3 Wavelet Soft Thresholding Based on CSDK

The new wavelet soft thresholding proposed in this paper can be expressed as follows:

$$\hat{w}_{i,j} = \begin{cases} \text{sign}(w_{i,j})(|w_{i,j}| - \lambda \mathfrak{R}(w_{i,j})), & \text{if } |w_{i,j}| \geq \lambda \\ 0, & \text{otherwise} \end{cases}$$

Where $w_{i,j}$ is wavelet coefficient and λ is a threshold value. So a new function curve is drawn in Figure 2.

The properties of the new function are as follows.

Theorem 1. *Continuity: There is no breakpoint, so $f(\text{new}_x)$ is a continuous function in its domain.*

Proof. From its curve, we can know the domain, and the range of the function is $(-\infty, +\infty)$.

When $x > \lambda$,

$$f(\text{new}_x) = \text{sign}(w_{i,j})(w_{i,j} - \lambda \mathfrak{R}(w_{i,j})).$$

Therefore, the right-hand limit of the function is:

$$\lim(f(\text{new}_x)_{x \rightarrow \lambda^+}) = x - \lambda e^0 = 0.$$

When $x < -\lambda$,

$$f(\text{new}_x) = \text{sign}(w_{i,j})(-w_{i,j} - \lambda \mathfrak{R}(w_{i,j})).$$

Therefore, the right-hand limit of the function is:

$$\lim(f(\text{new}_x)_{x \rightarrow \lambda^-}) = -x - \lambda e^0 = 0.$$

When $-\lambda \leq x \leq \lambda$

$$f(\text{new}_x) \equiv 0.$$

Considering the above formulas, $\lim(f(\text{new}_x)_{x \rightarrow \lambda^-}) = \lim(f(\text{new}_x)_{x \rightarrow \lambda^+}) = \lim(f(0))$.

Thus, the new function is a continuous curve in its domain. Moreover, it compensates for the shortcomings of the hard threshold function. \square

Theorem 2. *Monotonicity: $f(new_x)$ is a monotonically increasing function in $(-\infty, +\infty)$, so $f(new_x)$ is an increasing function in the domain of $(-\infty, +\infty)$.*

Proof. When $x > \lambda$,

$$f(new_x) = \text{sign}(w_{i,j})(x - \lambda e^{-\frac{[\alpha(x-\lambda)/\lambda-\mu]^2}{2\sigma^2}}).$$

The first derivative of $f(new_x)$ is:

$$f'(new_x) = 1 + \frac{2x\alpha^2}{e^{\alpha x^2}}.$$

Regardless of α , $f'(new_x) > 0$. We use the identical calculation method: if $x < -\lambda$, similarly, $f'(new_x) > 0$.

When $-\lambda \leq x \leq \lambda$

$$f(new_x) \equiv 0.$$

Therefore, $f(new_x)$, which is a monotonically increasing function, is proven. \square

Theorem 3. *Differentiability: $f(new_x)$ is differentiable.*

Proof. The new function is continuous and monotonic, and its right and left limits are equal. Thus, it is differentiable. \square

3.4 Optimized Threshold Parameter λ

As we know, parameter λ plays an important role in the wavelet threshold function. Donoho [9] proposed a common threshold formula,

$$\lambda = \varepsilon \sqrt{2 \log(N)}.$$

where ε is the noise variance, and N is the sampling length of the signal. When multiple wavelet decompositions for an image are analyzed, the noise amplitude notably decreases with the increase in the number of image layers. However, the amplitude of image information increases. Therefore, this paper proposes an optimized threshold parameter λ :

$$\lambda = \varepsilon \sqrt{2 \log(N) / \log(1 + e^j)}.$$

where j denotes the layer of image decomposition. In this formula, if j increases, the optimized λ gradually decreases. The improved λ is superior to that in some state-of-the-art functions.

Then, we study the effect of j on the new wavelet threshold function. When j is large, the effect of α is notably small, which can reduce the noise turbulence. Hence, our new function is effective.

3.5 Image Decryption

Image processing party will transform the encryption image with improved denoising algorithm to the image receiver. The image receiver is trusted by the sender with image decryption key. Therefore, it can decrypt the image successfully. After decrypting image, it is the denoised image.

4 Experiment and Analysis

In this section, experiments are conducted to demonstrate the effectiveness of the CSDK with MATLAB R2014b, Core i7 CPU, 8 GB memory and Windows 10 platform environment. In Section 4.1, the evaluation criterion and its function are introduced to evaluate our new method. First, we experimented with different parameter values in the new function and analyzed their effect on the wavelet threshold de-noising in Section 4.2. Then, we made a comparison to state-of-the-art threshold functions to verify the effectiveness of our new method in Section 4.3. All experiments were conducted using the same software, hardware and laptop.

The image evaluation criterion contains two aspects: subjective evaluation and objective evaluation. In this subsection, we mainly evaluate the new function with objective evaluation. In the new function, the shape parameter is adjusted to improve the effect on image de-noising. Two widely used indicators are employed to indicate the effect of image de-noising: the signal-to-noise-ratio (SNR), (normalized mean square error) NMSE and (Structural Similarity) SSIM.

4.1 Performance Evaluation of Different Parameters for Image De-noising

As we know, the shape parameter significantly affects the image de-noising. Thus, the shape parameter selection is notably important. According to the principle of Gaussian kernel function, $\alpha = 1$. First, we study the effect of μ and σ on the image de-noising. Assuming that $N = 30$, $\varepsilon = 0.6$, and $j = 0.2$, we selected "Lena", "Barbara", "Baboon" in international standard test images as the testing images. Figure 3 shows the original images and noisy images under Gaussian noise=0.04, 0.3, 0.7. These results are shown in Figures 4, 5, 6(a-i) only when Gaussian noise=0.04.

4.2 Effect of Parameter ε on Image De-noising

The analyzed parameters were manually optimized for the best peak SNR, which is the metric in our evaluation. Let $\mu = 0$, $j = 5$, $\sigma^2 = 0.1$, and $N = 30$ in this subsection. We conducted six experiments to study the effect of shape parameter on the trend of the SNR, which are listed in Tables 1, 2, and 3 (the fourth, fifth and sixth column denote the noise 0.04, 0.3 and 0.7 respectively). Obviously, with the increase in ε , the SNR of the new function is gradually reduced.

4.3 Comparison Experiments

In this subsection, we compare our method with state-of-the-art threshold functions (the wavelet based including soft threshold function, Reference [20] and Reference [21]) and other famous non-wavelet-based image de-

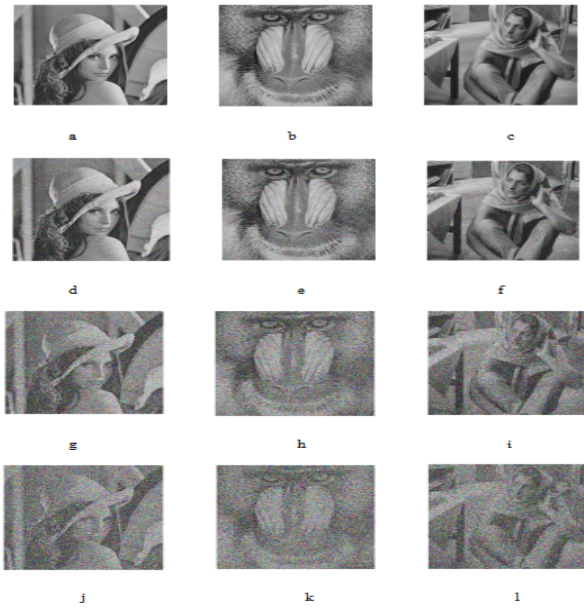


Figure 3: Testing images. Original images: (a) Lena, (b) Baboon, (c) Barbara; Noisy images with Gaussian noise=0.04: (d) Lena, (e) Baboon, (f) Barbara; Gaussian noise=0.3: (g) Lena, (h) Baboon, (i) Barbara; Gaussian noise=0.7: (j) Lena, (k) Baboon, (l) Barbara

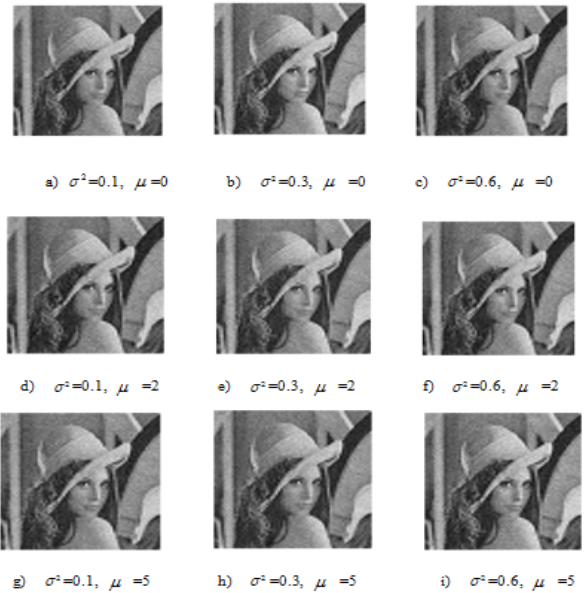


Figure 4: Image Lena de-noising with different σ and μ

Table 1: SNR values of Lina with different ϵ

N	P	SNR1	0.04	0.3	0.7
1	$\epsilon = 0.1$	8.8158	18.9769	17.6859	17.3247
2	$\epsilon = 0.2$	8.8052	18.9373	17.6321	17.2967
3	$\epsilon = 0.4$	8.7992	18.9638	17.5847	17.1169
4	$\epsilon = 0.6$	8.8120	18.9694	17.1365	17.0954
5	$\epsilon = 0.8$	8.8097	18.9351	16.5846	16.8796
6	$\epsilon = 0.9$	8.8241	18.9585	16.5787	16.8219

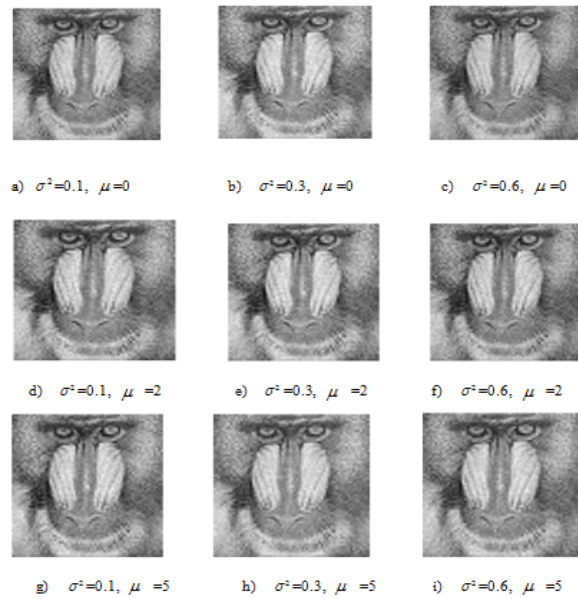


Figure 5: Image Baboon de-noising with different σ and μ



Figure 6: Image Barbara de-noising with different σ and μ

Table 2: SNR values of Barbara with different ϵ

N	P	SNR1	0.04	0.3	0.7
1	$\epsilon = 0.1$	8.1170	15.8529	14.6582	14.3213
2	$\epsilon = 0.2$	8.1024	15.8523	14.6108	14.3106
3	$\epsilon = 0.4$	8.0901	15.8218	14.5837	14.2885
4	$\epsilon = 0.6$	8.0823	15.8295	14.5086	14.1907
5	$\epsilon = 0.8$	8.0964	15.7821	14.4975	14.1537
6	$\epsilon = 0.9$	8.0942	15.8028	14.4617	14.0662

noising methods (Reference [13,17,22,29]) to demonstrate the effectiveness of our new method. In the simulated study, three images were used for testing: "Lena", "Baboon" and "Barbara".

In all experiments, the parameters of the references were set according to the above analysis: $\mu = 0$, $j = 5$, $\sigma^2 = 0.1$, $N = 30$, $\varepsilon = 0.1$, and $\alpha = 1$. They were used for all comparison experiments. We have extensively tested these values as the criteria for image de-noising and find them succeed in virtually all cases.

In Lena test experiment, the denoised image using the new method in Figure 7 is compared with the denoised image of other de-noising methods. As observed, the new method successfully eliminates noise and obtains more accurate results than other methods. Note that there are some spots in soft threshold function. Reference 24 method indicates that the de-noising effect has better smoothness, but the image is fuzzy.

Similarly, in Baboon and Barbara experiments (Figures 8 and 9), the new method effectively removes the baseline noise and can better retrieve the images compared to other de-noising methods.

Tables 4, 5 and 6 show the SNR, NMSE, SSIM of the original noisy and denoised image with different de-noising methods. According to table 7, SNR2, NMSE, SSIM with our new method are 18.9692, -8.8180 and 0.9846, which are the largest values among the methods; the soft threshold function has second largest SNR value (18.9387), followed by Reference [30] (18.8827) and Reference [17] (18.7109). Overall, the table shows that our new method can obtain better effect than the other methods.

Similarly, Tables 5 and 6 imply that the new method outperforms the current de-noising methods and successfully recovers the desired images. The values of SNR, NMSE, SSIM of the proposed adaptive de-noising algorithm are slightly higher than that of the other compared state-of-the-art methods. It shows that the proposed algorithm has a stronger ability to enhance the edges, the texture regions of the image, and preserve the smooth regions of the image while removing the noise.

5 Conclusion

This paper proposed a new image encryption and de-noising method, the image de-noising combines wavelet threshold function and the Chi-square distribution-Kernel function. In this paper, we discussed our new function including the relation between j and α and the effect of ε . Then, the proposed method was tested on three simulated images and made comparison with several other popular de-noising methods. Both numerical and visual results demonstrate that the proposed method in this article could strongly better remove most of the noise. Few image details were lost. The new algorithm could not only achieve the goal of removing noise, but prevented the image content leaking again, which effectively protected the image's security and privacy.



Figure 7: Image Lena de-noising results and experiment contrast. (a) Soft threshold; (b) reference [20]; (c) reference [21]; (d) reference [29]; (e) reference [13]; (f) reference [22]; (g) reference [17]; (h) the proposed CSDK

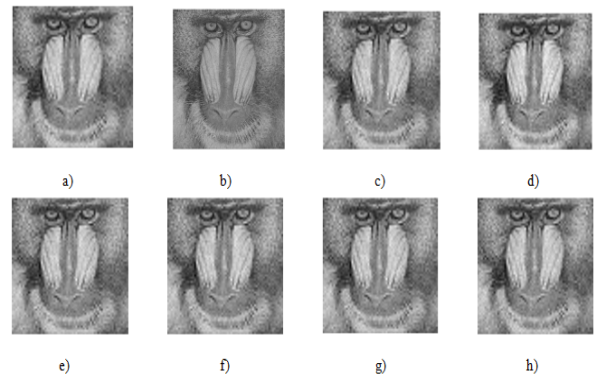


Figure 8: Image Baboon de-noising results and experiment contrast. (a) Soft threshold; (b) reference [20]; (c) reference [21]; (d) reference [29]; (e) reference [13]; (f) reference [22]; (g) reference [17]; (h) the proposed CSDK



Figure 9: Image Barbara de-noising results and experiment contrast. (a) Soft threshold; (b) reference [20]; (c) reference [21]; (d) reference [29]; (e) reference [13]; (f) reference [22]; (g) reference [17]; (h) the proposed CSDK

Acknowledgments

This work is supported by the Natural Science Fund Guiding Program in Liaoning Province (Grant No.20180520024).

References

- [1] J. Ai, X. Qi, W. Yu, *et al.*, "A new CFAR ship detection algorithm based on 2-D joint log-normal distribution in SAR images," *IEEE Geoscience & Remote Sensing Letters*, vol. 7, no. 4, pp. 806-810, 2010.
- [2] M. V. Aref'Eva, "Optimality of regularizing algorithms for the solution of stochastic operator equations," *Medical Image Analysis*, vol. 17, no. 8, pp. 1025-1036, 2013.
- [3] S. Beheshti, M. Hashemi, X. P. Zhang, *et al.*, "Noise invalidation denoising," *IEEE Transactions on Signal Processing*, vol. 58, no. 12, pp. 6007-6016, 2010.
- [4] R. G. Brereton, "The F distribution and its relationship to the chi squared and t distribution," *Journal of Chemometrics*, vol. 29, no. 11, pp. 582-586, 2015.
- [5] T. Y. Chang and M. S. Hwang, W. P. Yang, "An improved multi-stage secret sharing scheme based on the factorization problem," *Information Technology and Control*, vol. 40, no. 3, PP. 246-251, 2011.
- [6] S. F. Chiou, M. S. Hwang, S. K. Chong, "A simple and secure key agreement protocol to integrate a key distribution procedure into the DSS," *International Journal of Advancements in Computing Technology (IJACT'12)*, vol. 4, no. 19, pp. 529-535, Oct. 2012.
- [7] L. Dong, "Adaptive image denoising using wavelet thresholding," in *IEEE International Conference on Information Science and Technology*, pp. 854-857, 2013.
- [8] D. L. Donoho, I. M. Johnstone, "Adapting to unknown smoothness via wavelet shrinkage," *Journal of the American Statistical Association*, vol. 90, no. 432, pp. 1200-1224, 1995.
- [9] D. L. Donoho, I. M. Johnstone, G. Kerkycharian, *et al.*, "Density estimation by wavelet thresholding," *Annals of Statistics*, vol. 24, no. 2, pp. 508-539, 1996.
- [10] T. J. Hagey, J. B. Puthoff, K. E. Crandell, *et al.*, "Modeling observed animal performance using the Weibull distribution," *Journal of Experimental Biology*, vol. 219, no. 11, 2016.
- [11] C. Hensen, W. Schulz, "Time dependence of the channel characteristics of low voltage power-lines and its effects on hardware implementation," *AEU - International Journal of Electronics and Communications*, vol. 54, no. 1, pp. 23-32, 2000.
- [12] W. Hsien, C. C. Yang and M. S. Hwang, "A survey of public auditing for secure data storage in cloud computing," *International Journal of Network Security*, vol. 18, no. 1, pp. 133-142, 2016.
- [13] F. Huang, B. Lan, J. Tao, *et al.*, "A parallel nonlocal means algorithm for remote sensing image denoising on an intel xeon phi platform," *IEEE Access*, vol. 5, pp. 8559-8567, 2017.

Table 3: SNR values of Baboon with different ϵ

N	P	SNR1	0.04	0.3	0.7
1	$\epsilon = 0.1$	8.8960	14.2881	13.1968	12.9878
2	$\epsilon = 0.2$	8.9035	14.2825	13.1724	12.9673
3	$\epsilon = 0.4$	8.9075	14.2776	13.1309	12.8755
4	$\epsilon = 0.6$	8.9026	14.2662	13.0859	12.8106
5	$\epsilon = 0.8$	8.9001	14.2486	13.0554	12.7984
6	$\epsilon = 0.9$	8.9154	14.2672	12.9975	12.7763

Table 4: SNR values of Lena with different methods

Method	SNR1	SNR2	NMSE	SSIM
Soft threshold	8.8078	18.9387	-10.8537	0.7264
Reference [20]	14.4077	16.1786	-10.6529	0.7922
Reference [21]	8.2921	17.6859	-10.5649	0.7916
Reference [29]	8.6795	18.6653	-9.2416	0.8523
Reference [13]	8.3549	18.6941	-8.9761	0.8467
Reference [22]	8.5837	18.7109	-8.9178	0.8824
Reference [17]	8.6714	18.8827	-8.8596	0.8927
CSDK	8.7965	18.9692	-8.8180	0.9846

Table 5: SNR values of Baboon with different methods

Method	SNR1	SNR2	NMSE	SSIM
Soft threshold	8.9129	14.2760	-10.8795	0.8593
Reference [20]	8.5807	14.3085	-10.6547	0.8654
Reference [21]	8.2921	13.6859	-10.5466	0.8746
Reference [29]	8.3164	14.2128	-9.9762	0.8922
Reference [13]	8.3253	14.3107	-9.8524	0.9137
Reference [22]	8.5508	14.3193	-9.7688	0.9248
Reference [17]	8.5674	14.2984	-9.6417	0.9617
CSDK	8.9038	14.3692	-8.1251	0.9835

Table 6: SNR Values of Barbara With Different methods

Method	SNR1	SNR2	NMSE	SSIM
Soft threshold	8.5746	15.2381	-10.81537	0.8601
Reference [20]	8.6472	15.6812	-9.9054	0.8639
Reference [21]	8.3451	15.8787	-9.7822	0.8854
Reference [29]	8.3188	16.4827	-8.5897	0.9025
Reference [13]	8.2643	16.5374	-8.3074	0.9437
Reference [22]	8.7549	16.6548	-8.3576	0.9548
Reference [17]	8.7654	16.7876	-8.5917	0.9627
CSDK	8.9277	16.8763	-7.6548	0.9829

- [14] Y. Ji, D. Li, M. Yu, *et al.*, "A de-noising algorithm based on wavelet threshold-exponential adaptive window width-fitting for ground electrical source airborne transient electromagnetic signal," *Journal of Applied Geophysics*, vol. 128, pp. 1-7, 2016.
- [15] S. A. Kadhim, "A new signal de-noising method using adaptive wavelet threshold based on PSO algorithm and kurtosis measuring for residual noise," *Journal of Babylon University*, vol. 25, no. 1 pp. 8-19, 2017.
- [16] S. Khatoon, T. Thakur, B. Singh, "A provable secure and escrow-able authenticated group key agreement protocol without NAXOS trick," *International Journal of Computer Applications*, vol. 171, no. 3, pp. 1-8, 2017.
- [17] H. Li, C. Y. Suen, "A novel non-local means image denoising method based on grey theory," *Pattern Recognition*, vol. 49, pp. 237-248, 2016.
- [18] J. Liu, S. L. Yin, H. Li and L. Teng, "A density-based clustering method for k-anonymity privacy protection," *Journal of Information Hiding and Multimedia Signal Processing*, vol. 8, no. 1, pp. 12-18, Jan. 2017.
- [19] L. Liu, Z. Cao, C. Mao, "A note on one outsourcing scheme for big data access control in cloud," *International Journal of Electronics and Information Engineering*, vol. 9, no. 1, pp. 29-35, 2018.
- [20] J. Y. Lu, L. Hong, Y. Dong, *et al.*, "A new wavelet threshold function and denoising application," *Mathematical Problems in Engineering*, vol. 3, pp. 1-8, 2016.
- [21] M. Srivastava, C. L. Anderson, J. H. Freed, "A new wavelet denoising method for selecting decomposition levels and noise thresholds," *IEEE Access Practical Innovations Open Solutions*, vol. 4, pp. 3862, 2016.
- [22] L. Teng, H. Li, S. Yin, "Modified pyramid dual tree direction filter-based image denoising via curvature scale and nonlocal mean multigrade remnant filter," *International Journal of Communication Systems*, vol. 3, 2017. DOI: 10.1002/dac.3486
- [23] D. Wang, H. Lu, M. H. Yang, "Least soft-threshold squares tracking," in *IEEE Computer Vision and Pattern Recognition*, pp. 2371-2378, 2013.
- [24] Q. Wang, H. Wen, Y. Han, *et al.*, "The research and application of image de-noising based on the improved method of wavelet thresholding," in *International Conference on Intelligent Earth Observing and Applications*, 98083U, 2015. (<https://doi.org/10.1117/12.2206149>)
- [25] Y. Wu, H. Tan, Y. Li, *et al.*, "Robust tensor decomposition based on Cauchy distribution and its applications," *Neurocomputing*, no. 223, pp. 107-117, 2017.
- [26] Q. Xu, Q. Chen, S. Yang, *et al.*, "Superpixel-based classification using K distribution and spatial context for polarimetric SAR images," *Remote Sensing*, vol. 8, no. 8, pp. 619, 2016.
- [27] S. L. Yin and J. Liu, "A k-means approach for map-reduce model and social network privacy protection," *Journal of Information Hiding and Multimedia Signal Processing*, vol. 7, no. 6, pp. 1215-1221, Nov. 2016.
- [28] S. Yin, L. Teng, J. Liu, "Distributed searchable asymmetric encryption," *Indonesian Journal of Electrical Engineering and Computer Science*, vol. 4, no. 3, pp. 684-694, 2016.
- [29] J. Yu, L. Tan, S. Zhou, *et al.*, "Image denoising algorithm based on entropy and adaptive fractional order calculus operator," *IEEE Access*, vol. 5, pp. 12275-12285, 2017.
- [30] Q. Zhang, L. T. Yang, X. Liu, Z. Chen, and P. Li, "A tucker deep computation model for mobile multimedia feature learning," *ACM Transactions on Multimedia Computing, Communications and Applications*, vol. 13, no. 3, pp. 1-39:18, 2017.

Biography

Lin Teng received the B.Eng. degree from Shenyang Normal University, Shenyang, Liaoning province, China in 2016. Now, she is a laboratory assistant in Shenyang Normal University. Her research interests include Multimedia Security, Network Security, Filter Algorithm and Data Mining. She had published more than 10 international journal papers on the above research fields. Email:1532554069@qq.com.

Jie Liu is a full professor in Software College, Shenyang Normal University. He received his B.S. and M.S. degrees from Harbin Institute of Technology. He is also a master's supervisor. He has research interests in wireless networks, mobile computing, cloud computing, social networks, network security and quantum cryptography. Professor Liu had published more than 30 international journal papers (SCI or EI journals) on the above research fields. Email: nan127@sohu.com.

Shoulin Yin received the B.Eng. degree from Shenyang Normal University, Shenyang, Liaoning province, China in 2016. Now, he is a doctor in Harbin Institute of Technology. His research interests include Multimedia Security, Network Security, image processing and Data Mining. Email:352720214@qq.com.

Yang Sun obtained his master degree in Information Science and Engineering from Northeastern University. Yang Sun is a full associate professor of the Kexin software college at Shenyang Normal University. He is also a department head of network engineering. He has research interests in wireless networks, mobile computing, cloud computing, social networks and network security. Yang Sun had published more than 15 international journal and conference papers on the above research fields.